Environmental Science & Technology

Article

pubs.acs.org/est

# New Evidence for High Sorption Capacity of Hydrochar for Hydrophobic Organic Pollutants

Lanfang Han,[†,∥] Kyoung S. Ro,[‡] Ke Sun,*[,†] Haoran Sun,[†] Ziying Wang,[†] Judy A. Libra,[§] and Baoshan Xing[∥]

[†]State Key Laboratory of Water Environment Simulation, School of Environment, Beijing Normal University, Beijing 100875, China

[‡]Coastal Plains Soil, Water, and Plant Research Center, Agricultural Research Service, U.S. Department of Agriculture, 2611 West Lucas Street, Florence, South Carolina 29501, United States

[§]Leibniz Institute for Agricultural Engineering, Max-Eyth-Allee 100, 14469 Potsdam-Bornim, Germany

[∥]Stockbridge School of Agriculture, University of Massachusetts, Amherst, Massachusetts 01003, United States

Supporting Information

**ABSTRACT:** This study investigated the sorption potential of hydrochars, produced from hydrothermally carbonizing livestock wastes, toward organic pollutants (OPs) with a wide range of hydrophobicity, and compared their sorption capacity with that of pyrochars obtained from conventional dry pyrolysis from the same feedstock. Results of SEM, Raman, and $^{13}$C NMR demonstrated that organic carbon (OC) of hydrochars mainly consisted of amorphous alkyl and aryl C. Hydrochars exhibited consistently higher log $K_{oc}$ of both nonpolar and polar OPs than pyrochars. This, combined with the significantly less energy required for the hydrothermal process, suggests that hydrothermal conversion of surplus livestock waste into value-added sorbents could be an alternative manure management strategy. Moreover, the hydrochars log $K_{oc}$ values were practically unchanged after the removal of amorphous aromatics, implying that amorphous aromatic C played a comparable role in the high sorption capacity of hydrochars compared to amorphous alkyl C. It was thus concluded that the dominant amorphous C associated with both alkyl and aryl moieties within hydrochars explained their high sorption capacity for OPs. This research not only indicates that animal-manure-derived hydrochars are promising sorbents for environmental applications but casts new light on mechanisms underlying the high sorption capacity of hydrochars for both nonpolar and polar OPs.

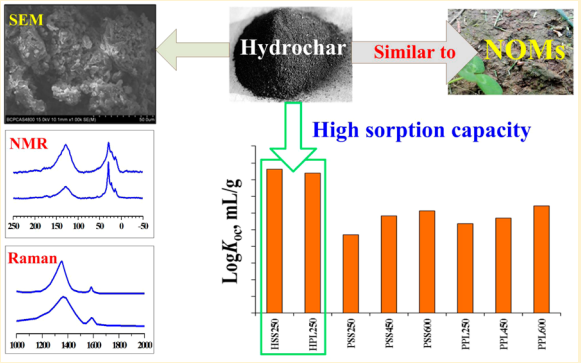


## INTRODUCTION

Biochar, an emerging carbon (C) material derived from renewable resources (e.g., biomass, agricultural crop residues, and livestock wastes),[1] has triggered a new "gold rush" based on its broad practical applications in a variety of areas, covering C sequestration, potential soil amendments and environmental remediation.[2,3] Biochars made via dry pyrolysis (referred to as pyrochars) from woody feedstocks have been studied for decades as sorbents in environmental remediation.[4,5] There is a general consensus that the physicochemical heterogeneity of biochars is governed by feedstock sources along with pyrolysis process conditions.[6] Few studies, however, have been made on biochars from less traditional feedstocks such as livestock wastes or those produced via wet pyrolysis or hydrothermal carbonization (HTC).[7,8] Depending upon the process conditions used, the C recovery of HTC can be very high, and the majority of the initial C stays bound in the final carbonaceous material (so-called hydrochars).[8−10] In contrast to conventional dry pyrolysis, HTC can process wet biomass without a prior drying step. Although the solids may need to be separated and dried after the HTC process, the ease of dewatering is increased, which reduces energy requirements for the drying process. As a result, HTC requires significantly less energy than conventional dry pyrolysis.[11] Additionally, due to the different processing conditions experienced by hydrochars and pyrochars, their chemical structures can differ significantly, which has been underscored in numerous studies, e.g., Titirici and Antonietti,[8] Titirici et al.,[12] and Cao et al.[13] Since chemical composition, physical conformation, and polarity of natural organic sorbents in soils and sediments as well as man-made biochars have been shown to affect organic compound sorption,[14,15] the diverse structures of hydrochars and pyrochars possibly contribute to their different sorption abilities. Sun et al.[16] reported that the hydrochars derived from poultry litter and swine solids exhibited similar or higher

Received: May 13, 2016
Revised: November 4, 2016
Accepted: November 22, 2016
Published: November 22, 2016





DOI: 10.1021/acs.est.6b02401
Environ. Sci. Technol. 2016, 50, 13274−13282

sorption capacity toward bisphenol A, 17a-ethinyl estradiol, and phenanthrene than the pyrochars produced from pyrolyzing poultry litter and wheat straw at 400 °C. These findings imply that hydrochar could be utilized as valuable sorbents. However, the feedstocks for the hydrochars and pyrochars were different. Therefore, it is difficult to draw any meaningful comparison. More importantly, the potential mechanism underlying the high sorption capacity of hydrochars was not addressed.

The HTC process was first used to simulate coal-forming geological environments. Typical experimental HTC conditions (150−350 °C under saturated water vapor pressure) are quite similar to those used to simulate the diagenesis of natural organic matter (NOM) in soils.[13,17] Wu et al.[18] have reported that cellulose-derived hydrochar was analogous to naturally occurring kerogen, organic carbon (OC) that is not soluble in acid, base, and organic solvents. Therefore, hydrochar from the HTC process, in essence, could play a role similar to NOM in soils. NOM has been already identified as the key soil components in adsorbing a wide range of hydrophobic organic compounds (HOCs) in soils.[14,15,19] In addition, the important role of alkyl domains within NOM in the interaction with HOCs has been highlighted in extensive studies.[19−22] In previous research,[14] we selected humic acids, humins, and nonhydrolyzable organic carbon (NHC, i.e., nonhydrolyzable residue after the treatment with trifluoroacetic acid (TFA) and HCl) as representatives of NOM and clearly demonstrated that it was the alkyl C rather than aromatic C that regulated the sorption of HOCs by NOM. On the basis of this, we hypothesized that just like NOM, hydrochars may have the potential to efficiently remove the HOCs in soils or wastewaters, and the alkyl moieties of hydrochar may be responsible for its sorption behavior.

The major objectives of this study were therefore to (1) evaluate the potential of hydrochars in removing selected organic contaminants with a wide range of log $K_{ow}$ and compare the sorption capacity of hydrochars and pyrochars derived from the same feedstock and (2) explore the mechanisms accounting for their high sorption capacity. To achieve these goals, the physicochemical structures of hydrochars and pyrochars were characterized using X-ray photoelectron spectra (XPS), scanning electron microscopy (SEM), Raman spectra, and solid-state cross-polarization magic-angle-spinning $^{13}C$ nuclear magnetic resonance spectra ($^{13}C$ CP-MAS NMR). Pyrene (PYE) and four pharmaceuticals and personal care products (PPCPs) (triclosan (TCS), estrone (E1), carbamazepine (CBZ), and acetaminophen (AMP)) were selected as sorbates to span a wide range of hydrophobicity.

## MATERIALS AND METHODS

**Sorbates and Sorbents.** PYE (97+%), TCS (99+%), E1 (99+%), CBZ (99+%), and AMP (99+%) were used as sorbates and obtained from Sigma-Aldrich Chemical Co. Selected physicochemical properties of five chemicals are summarized in Table S1. The preparation methods of hydrochars and pyrochars from swine solids and poultry litter were described elsewhere.[23] Briefly, hydrochars were prepared by hydrothermally carbonizing swine solids or poultry litter at 250 °C. Dried and ground (less than 2 mm) swine solids and poultry litter were mixed with distilled (DI) water to obtain a slurry of 20% (w/w) solids. This slurry was placed into a 1-L nonstirred T316 stainless steel reactor with an external heater (Parr Instruments, Moline, IL). The operating pressure of the system ranged from 3.4 to 9.0 MPa, representing subcritical conditions. Afterward, the reactor was cooled to room temperature before the reaction products were filtered and dried at 105 °C. Subsequently, swine-solid- and poultry-litter-derived hydrochars were washed with DI water (denoted as HSS250 and HPL250, respectively). After drying at 105 °C, HSS250 and HPL250 were gently ground and homogenized to pass through a 0.25 mm sieve. For pyrochars, swine solids and poultry litter with a prior drying treatment were carbonized at 250, 450, 600 °C for 4 h under $N_2$ conditions in a Lindburg electric box furnace equipped with a gastight retort (Model 51662; Lindburg/MPH, Riverside, MI). The temperature control of the retort system was based on input temperatures allowing for accurate control of pyrolytic exposure temperature. The HTTs were raised to the desired values (250, 450, and 600 °C) at a ramp rate of about 8 °C/min. The pyrochars were washed with DI water and subsequently oven-dried at 105 °C. Then, these pyrochars were gently ground and homogenized to pass through a 0.25 mm sieve. The pyrochars are hereafter referred to by their abbreviations based on their individual initial capitals of feedstock source and HTTs (i.e., PSS250, PSS450, PSS600, PPL250, PPL450, and PPL600).

The bleaching (BL) procedure, which was used to remove the noncondensed aromatic C (e.g., such as lignin-like and polyphenol units) of samples, was described in detail elsewhere.[24] Briefly, the bleaching involved treating 1 g of each sorbent three times (7 h for each time) with 10 g of sodium chlorite ($NaClO_2$), 10 mL of acetic acid ($CH_3COOH$) and 100 mL of DI water. All BL samples (i.e., HSS250-BL, HPL250-BL, PSS250-BL, PSS450-BL, PSS600-BL, PPL250-BL, PPL450-BL, and PPL600-BL) were freeze-dried, ground, and stored for their characterization and sorption work.

**Sorbent Characterization.** The bulk OC, H, N, and O compositions of all samples were determined with an Elementar Vario ELIII elemental analyzer via complete combustion. Ash content of biochars was measured by heating samples at 750 °C for 4 h.[25] X-ray photoelectron spectra (XPS), which can provide specific information on the surface elemental composition (depth: 3−5 nm) of samples and analysis of large sections (about 100 $\mu$m) of the particles, were recorded with a Kratos Axis Ultra electron spectrometer using a monochromated Al K$\alpha$ source operated at 225 W. Processing of the spectra was accomplished with the Xpspeak41 software. Four components were identified and quantified in the C 1s spectra: 284.8 eV (representing C−C and C−H bonds), 286.3 eV (C−O bonds), 287.5 eV (C═O bonds), and 289.0 eV (COOH bonds). The particle structure and surface topography of hydrochars and pyrochars were investigated using SEM imaging analysis with a Hitachi S4800 scanning microscope (Japan). $^{13}C$ CP-MAS NMR spectra of biochars were obtained using a Bruker Avance 300 NMR spectrometer (Karlsruhe, Germany) for structural composition. The NMR running parameters and chemical shift assignments were depicted elsewhere.[19] Raman measurements of samples were performed on a Labram aramis excited with a 532 nm laser. Pore and surface characteristics were examined by gas ($N_2$ and $CO_2$) adsorption using an Autosorb-1 gas analyzer (Quantachrome Instrument Corp., Boynton Beach, FL). Surface area (SA) using a $CO_2$ isotherm at 273 K was calculated using nonlocal density functional theory (NLDFT; Figure S1). The SA using $N_2$ was determined by the Brunaer−Emmett−Teller (BET) equation with multipoint adsorption isotherms of $N_2$ at 77 K.

**Sorption Experiments.** All sorption isotherms were obtained using a batch equilibration technique at 23 ± 1 °C.


DOI: 10.1021/acs.est.6b02401
Environ. Sci. Technol. 2016, 50, 13274−13282

An appropriate amount of the investigated biochar samples was added to the background solution, which contained 0.01 M $CaCl_2$ in DI water with 200 mg/L $NaN_3$ to minimize biodegradation. The amount of sorbents was chosen to result in 20−80% uptake of the initial solute amount. The solutes were added to the vials to achieve initial concentrations from 0.001 to 0.12 mg/L for PYE, 0.1 to 10 mg/L for TCS, 0.2 to 20 mg/L for E1, and 0.2 to 100 mg/L for both CBZ and AMP, in order to cover the range between detection limit and aqueous solubility of solutes. Our preliminary test indicated that apparent equilibrium of PYE, TCS, E1, and CBZ was reached within 7 days for hydrochars and pyrochars, while AMP reached apparent equilibrium within 2 days. The blank experiments included solute without any sorbent and sorbent without solute. Headspace was kept to a minimum to reduce solute vapor loss. After being shaken on the rotary shaker for 9 days of PYE, TCS, E1, and CBZ and for 3 days for AMP, all vials were placed upright for 24 h. Then, about 2 mL of supernatant was taken out and analyzed directly by HPLC (1260 Series, Agilent Technologies, Santa Clara, CA) equipped with a reversed-phase C18 column (5 $\mu$m, 4.6 mm × 250 mm). The concentration of PYE was analyzed with a fluorescence detector at 272 nm (excitation wavelength) and 419 nm (emission wavelength), while the investigated PPCPs were quantified on a diode array detector operated at a wavelength of 220 nm for TCS, 280 nm for E1, 280 nm for CBZ, and 249 nm for AMP. The mobile phases for the sorbates were PYE, methanol/water (90/10, v:v); TCS, acetonitrile/water (80/20, v:v); E1 and CBZ, acetonitrile/water (70/30, v:v); and AMP, acetonitrile/water (60/40, v:v). The flow rates for all sorbates were 0.8 mL/min, and the column temperature was set at 35 °C. All samples coupled with blanks were conducted in duplicate. The analysis of blank experiments showed that the sorption of each sorbate by the vials and the decomposition of each sorbate were insignificant, and the concentration of each sorbate potentially released from hydrochars and pyrochars was all below the detection limit.

**Data Analysis.** The sorption data were fitted to the logarithmic form of the Freundlich isotherm:

$$\log q_e = \log K_F + n \log C_e \quad (1)$$

where $q_e$ [$\mu$g/g] is the solid phase concentration, $C_e$ [$\mu$g/L] is the solution phase concentration, $K_F$ [($\mu$g/g)/($\mu$g/L)$^n$] is the Freundlich affinity coefficient, and $n$ is the Freundlich exponential coefficient.

The sorption distribution coefficient ($K_d$) and the OC-normalized $K_d$ ($K_{oc}$) were obtained with eqs 2 and 3.

$$K_d = q_e/C_e \quad (2)$$

$$K_{oc} = K_d/f_{oc} \quad (3)$$

where $f_{oc}$ is OC content. The log $K_d$ and log $K_{oc}$ values ($C_e$ = 0.01, 0.1, and 1$S_w$, water solubility of solutes) of hydrochars and pyrochars were calculated according to the above equations. The investigated correlations among properties of sorbents as well as their sorption coefficients of each sorbate (Pearson correlation coefficients: $p$ and $r$ values) were obtained from the Pearson correlation analysis with SPSS 16.0 software (SPSS Inc., USA).

## RESULTS AND DISCUSSION

**Characterization of Hydrochars and Pyrochars.** The bulk elemental composition, ash content, and SA determined by $CO_2$ ($CO_2$−SA) and $N_2$ ($N_2$−SA) of hydrochars and pyrochars are tabulated in Table S2. It has often been reported that the bulk C content of plant-derived pyrochars generally rises with HTTs.[6,26] However, manure-derived pyrochars in our study, which had high ash contents, did not follow this pattern. The pyrochars obtained at 250 °C contained more C than ones at 450 and 600 °C (Table S2). This was probably due to higher rates of loss for C-containing compounds relative to the ash components during pyrolysis, since the ash content was approximately doubled at the higher HTTs (Table S2). The OC contents of hydrochars were similar to (HPL250) or slightly higher (HSS250) than their corresponding pyrochars at 250 °C (PSS250 and PPL250). However, the typical van Krevelen diagram showed that they differed in the relationships between the H/C versus O/C atomic ratios (Figure 1).

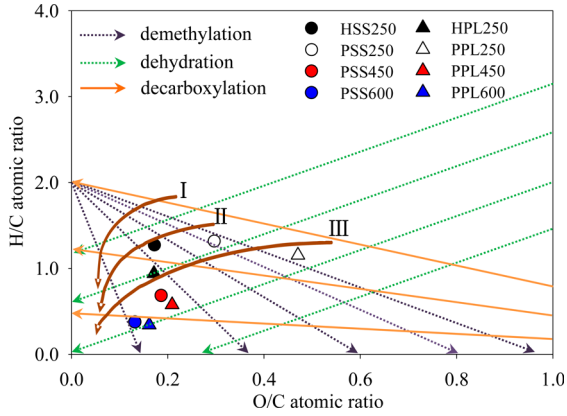


**Figure 1.** Van Krevelen plot of elemental ratios for swine-solid- and poultry-litter-derived hydrochars and pyrochars. Note that I, II, and III are three evolution paths of kerogen. H and P represent hydrochars and pyrochars, respectively. SS and PL refer to the biochars obtained from swine solids and poultry litter, respectively; 250, 450, and 600 are the heating treatment temperatures (°C).

Although the H/C ratios of two hydrochars were only slightly lower than corresponding pyrochars prepared at 250 °C, the O/C ratios were distinctly lower (Figure 1), indicating a higher degree of decarboxylation of hydrochars, which was further confirmed by the $^{13}C$ NMR analyses discussed below. The typical transition from the high ratios of H/C and O/C of the primary plant macromolecules (e.g., cellulose) to the low ratios of more carbonized structures[4,6,26] was seen for the pyrochars at 450 and 600 °C (Figure 1), suggesting that both feedstocks underwent substantial carbonization during the pyrolysis carried out at 450 and 600 °C. In contrast to conventional dry pyrolysis, the experimental conditions required by HTC are close to the real geological environment with moisture and are similar to those of the method used to simulate the diagenesis of NOM in soils.[17] From the van Krevelen diagram (Figure 1), it was seen that the elemental compositions of HSS250 and HPL250 were similar to those of type II and type III kerogen, respectively, which accorded well with the report by Wu et al.[18] that cellulose-derived hydrochar was analogous to naturally occurring kerogen. In addition, the aforementioned OC content and H/C ratios are important parameters in the International Biochar Initiative (IBI) guidelines[27] and European


DOI: 10.1021/acs.est.6b02401
Environ. Sci. Technol. 2016, 50, 13274−13282

biochar guidelines.[28] Concerning their OC content, all hydrochars and pyrochars belonged to class 2 biochar (30% ≤ OC content < 60%) according to the IBI guidelines. The molar ratios of H/C of 450 and 600 °C pyrochars were also lower than the maximum allowable threshold (0.7) required by IBI guidelines and European biochar guidelines. However, the H/C of hydrochars and 250 °C pyrochars did not meet the requirements. In general, the ratio of H/C is related to aromaticity and has thus been commonly proposed as an indicator of the relative stability of biochars in the soil system.[29,30] The biochars with a H/C higher than 0.7 may be considered to be labile or easily decomposed. However, there is emerging evidence that shows the H/C ratio or aromaticity level is not a unique factor determining the stability of biochars, and other factors (e.g., minerals) can exert an additional influence on its stability.[31−33] Moreover, there have been studies showing that the OC in hydrochar is more stable than we expect.[34] For instance, Malghani et al.[34] reported that roughly two-thirds of hydrochar remained in the soil after two cropping seasons. Further studies on matching biochar characteristics to its behavior in soils as well as longer term field trials are needed.

Table S3 shows the surface elemental compositions of two types of biochars. The surface O/C ratios of HSS250 (0.21) and HPL250 (0.49) were in the same range or lower than that of their corresponding pyrochars (0.22−0.42 and 0.40−0.67, respectively). Also, hydrochars generally contained less surface O-containing functional groups (C−O, C═O, and COOH) than the corresponding pyrochars, implying the relatively higher surface hydrophobicity of hydrochars.

SEM images in Figure 2 neatly display the dramatically different morphological characteristics of hydrochars and pyrochars. The hydrochar particles (HSS250 and HPL250) were relatively small in size and occurred as discrete spheres or as aciniform agglomerates (Figure 2), indicative of the amorphous structure of hydrochars.[35] A similar morphology was not observed in pyrochars (Figure 2). Compared with hydrochars, the surfaces of pyrochars were more inerratic and became flatter with the increase of HTTs. Moreover, the Raman spectra in Figure 3a and b illustrated that HSS250 and HPL250 mainly exhibited the amorphous C peak (1357 $cm^{-1}$), further demonstrating that the OC of hydrochars was primarily amorphous. For pyrochars, the influence of HTTs upon their crystallinity was observed (Figure 3). Specifically, only a small amorphous C peak was present for the 250 °C pyrochars, whereas the 450 and 600 °C pyrochars exhibited two typical peaks, namely, amorphous C (A) and graphite peak (G).[36] The A peak of the 450 °C pyrochars was comparable to or slightly stronger than their G peak, while the G peak of the 600 °C pyrochars was obviously sharper than their A peak (Figure 3a and b). The reason why only an amorphous carbon peak was observed may be related to the alteration of crystallinity of biochars with HTTs. During the pyrolytic process, the crystallinity of precursor carbon materials in feedstocks was lost around 250−300 °C.[6,37] For example, Keiluweit et al.[6] found that as the temperature increased from 100 to 300 °C, the crystallinity of precursor materials gradually decreased until it disappeared completely. With the loss of crystalline C, the amorphous C was gradually formed. Largely because of this process, 250 °C pyrochars in this study were mainly composed of amorphous C.

Besides the distinct morphology, $^{13}C$ NMR spectra (Figure 4 and Table S4) further showed that hydrochars and low and high temperature pyrochars were different in functional groups. The NMR spectra of hydrochars, being mainly composed of alkyl C (0−45 ppm) and aryl C (108−148 ppm), were largely

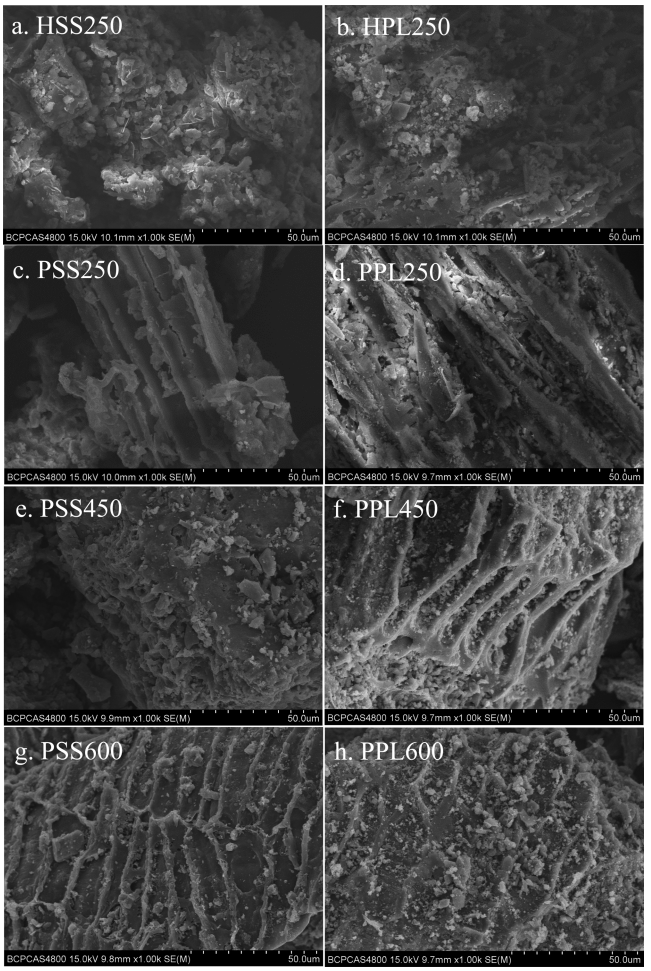


**Figure 2.** Scanning electron microscope (SEM) images of swine-solid- and poultry-litter-derived hydrochars and pyrochars. Note that H and P represent hydrochars and pyrochars, respectively. SS and PL refer to the biochars obtained from swine solids and poultry litter, respectively; 250, 450, and 600 are the heating treatment temperatures (°C).

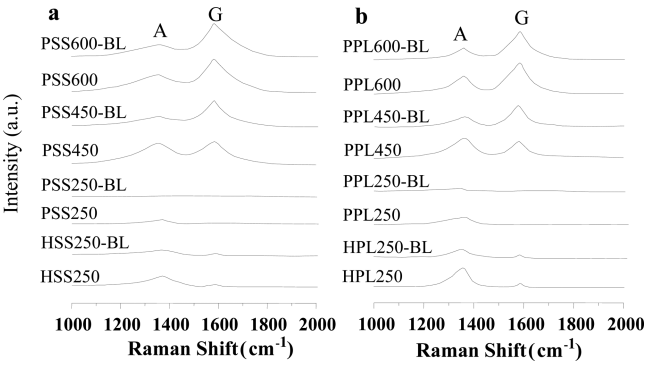


**Figure 3.** Comparison of Raman spectra of original and bleached swine-solid- (a) and poultry-litter-derived (b) hydrochars and pyrochars. Note that A and G refer to amorphous and graphite peaks, respectively. H and P represent hydrochars and pyrochars, respectively. SS and PL refer to the biochars obtained from swine solids and poultry litter, respectively; 250, 450, and 600 are the heating treatment temperatures (°C). "BL" denotes that the bleached samples.



DOI: 10.1021/acs.est.6b02401
Environ. Sci. Technol. 2016, 50, 13274−13282

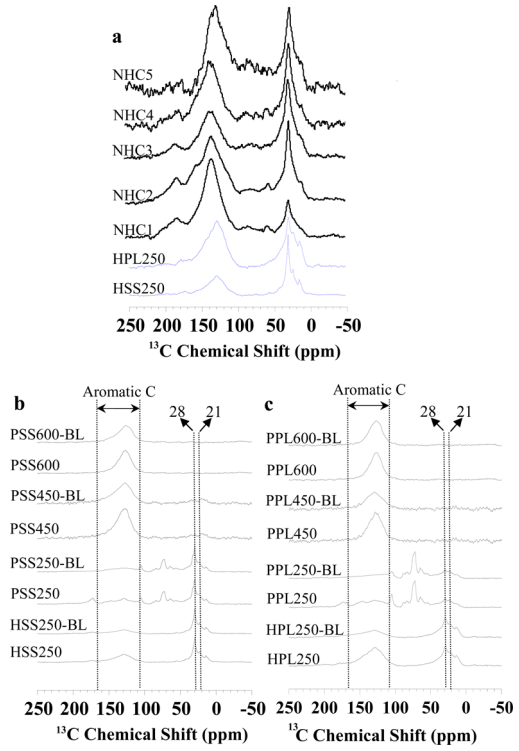


**Figure 4.** Comparison of solid-state $^{13}C$ CP-MAS NMR spectra of nonhydrolyzable carbon (NHC) (a) and original and bleached swine-solid- (b) and poultry-litter-derived (c) hydrochars and pyrochars. Note that NHC1 and NHC2 were NHC extracted from surface soils; NHC3, NHC4, and NHC5 were NHC extracted from sediments (data of NHC are cited from the report by Ran et al.[19]). H and P represent hydrochars and pyrochars, respectively. SS and PL refer to the biochars obtained from swine solids and poultry litter, respectively; 250, 450, and 600 are the heating treatment temperatures (°C). "BL" denotes that the bleached samples.

similar to those of NHC in soils and sediments (Figure 4a) studied by Ran et al.[19] and those of kerogen isolated from the Borden aquifer,[38] from the unweathered Woodford shale,[39] and from the Altrium shales.[40] Moreover, Ran et al.[41] have previously proposed that the $^{13}C$ NMR spectrum of NHC was similar to that of kerogen, and NHC was operationally similar to the kerogen. These results coincided well with the above-mentioned similar elemental compositions between hydrochars and type II and type III kerogen. Furthermore, the broad peak of 0−45 ppm of hydrochars belonged to short chain polymethylene (28 ppm) and methyl C in acetyl groups (21 ppm). These peaks all belong to amorphous aliphatic C.[21,42,43] No clear crystalline alkyl C peak (31.5 ppm) was observed in hydrochars. This was in satisfactory accordance with the amorphous OC structure of hydrochars suggested by SEM and Raman analyses. Additionally, consistent with the different elemental compositions of 250 °C pyrochars and 450 and 600 °C ones, they also contained different OC-containing functional groups. Specifically, pyrochars obtained at 250 °C (PSS250 and PPL250) had diverse functional groups including carbohydrates besides alkyl and aryl C, while pyrochars produced at high HTTs (450 and 600 °C) showed a large contribution of aromatic C (108−165 ppm) and a negligible contribution of alkyl C (0−45 ppm) and other structural groups (Figure 4b and c).[16,26] In view of the highly different compositions and structures, the 250 °C pyrochars could be differentiated from those produced at higher temperatures.

**Comparison of PYE and PPCPs Sorption between Hydrochars and Pyrochars.** The sorption isotherms of PYE and four PPCPs (TCS, E1, CBZ, and AMP) by hydrochars and pyrochars are shown in Figure S2, and the sorption data were well fitted with the Freundlich model as indicated by the high $R^2$ values (all >0.80; Tables S5−S9). Apart from pyrochars produced at 250 °C, all sorption isotherms of PYE and four PPCPs were highly nonlinear as evidenced by the nonlinear coefficient ($n$) ranging from 0.22 to 0.83 (Tables S5−S9). The sorption nonlinearity of hydrochars was higher than pyrochars prepared at 250 °C but weaker than pyrochars at 450 and 600 °C (Tables S5−S9); for pyrochars, the values of $n$ exhibited a downward trend with increasing HTTs. Figure S3a clearly indicated that the differing nonlinearity could be interpreted as the result of their different levels of aromaticity, with $n$ and aromaticity showing an inverse relationship. It has also been postulated that as more molecules entered into micropores, the isotherms became more nonlinear.[44] Using $CO_2$−SA as a measure of the microporosity, it could be seen that there is a significantly negative relationship between microporosity and the nonlinearity index $n$ values of PYE and PPCPs (Figure S3b). This relationship, along with the positive and significant correlation of $CO_2$−SA of pyrochars to their aromaticity, suggests the pore filling resulting from the nanopores from aromatic C dominates the nonlinear sorption of these selected sorbates by pyrochars.

The log $K_{oc}$ values of PYE, TCS, E1, CBZ, and AMP for each biochar followed the order at all test solute concentrations: PYE > TCS > E1 > CBZ > AMP, corresponding well to the order of their $K_{ow}$ values (Table S1). This suggests the role of hydrophobic effect (van der Waals force) in the sorption of tested sorbates by each biochar.[16,45] Previous work showed that the hydrochars prepared from swine solids and poultry litter at 250 °C displayed higher sorption to polar compounds (bisphenol A and 17a-ethinyl estradiol) than the pyrochars produced from wheat straw and poultry litter at 400 °C.[16] In the current study, it was found that when using the same feedstock source, hydrochars produced at 250 °C in the presence of water also exhibited higher sorption capacity to both nonpolar (PYE) and polar compounds (TCS, E1, CBZ, and AMP) than corresponding pyrochars obtained at low and high HTTs (250, 450, and 600 °C, respectively; Figure 5). For

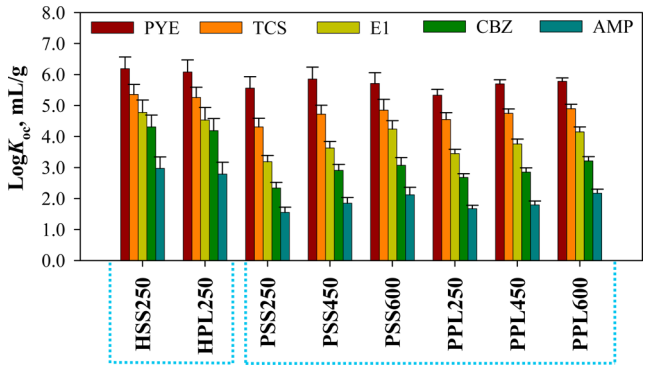


**Figure 5.** Comparison of log $K_{oc}$ between hydrochars and pyrochars for five sorbates including pyrene (PYE), triclosan (TCS), estrone (E1), carbamazepine (CBZ), and acetaminophen (AMP). Note that H and P represent hydrochars and pyrochars, respectively. SS and PL refer to the biochars obtained from swine solids and poultry litter, respectively; 250, 450, and 600 are the heating treatment temperature (°C).


DOI: 10.1021/acs.est.6b02401
Environ. Sci. Technol. 2016, 50, 13274−13282

instance, log $K_{oc}$ values ($C_e$ = 0.01$S_w$) of CBZ were in the range of 4.19 to 4.31 for hydrochars compared to 2.34 to 3.21 for pyrochars (Table S8). Moreover, the log $K_{oc}$ of PYE for hydrochars (6.08−6.19) in this investigation was also higher than those for plant-derived pyrochars at low and high HTTs.[46,47] However, in contrast to the high sorption capacity of hydrochars for TCS in this study, Zhu et al.[48] reported that the TCS adsorption capacity onto the plant-derived hydrochars at a similar temperature was low. The different results may be related to the different kind of feedstock used for hydrochar production. It has been largely reported that feedstock source is one of the key factors influencing the composition and structure of the final biochars, thereby affecting their sorption capacities.[49,50] Qiu et al.[26] observed that due to the much higher surface OC content than bulk OC of animal-manure-derived pyrochars, they exhibited higher sorption of dibutyl phthalate and phenanthrene compared to the plant-derived hydrochars. The animal-manure-derived hydrochars in this work showed much lower O contents (8.95−12.51%) than plant-derived ones (27.2%) reported by Zhu et al.,[48] which may partly explain the higher sorption capacities of hydrochars in this study to TCS. Therefore, animal-manure-derived hydrochars could be effective sorbents for environmental remediation. However, biochar itself may be considered as one type of potential contaminant; metals/metalloids and polycyclic aromatic hydrocarbons (PAHs)) within hydrochars and pyrochars should be compared before using hydrochars instead of pyrochars for remediation purposes. For metals/metalloids, it has been demonstrated that metal/metalloid concentrations depended on feedstocks of biochars, while HTTs exerted very little influence.[51] In this respect, hydrochars and pyrochars from swine solids or poultry litter in this study may have comparable metal/metalloid concentrations. For PAHs, their content and composition in the biochars were found to strongly depend on HTTs.[51] However, a large amount of PAHs within biochars were observed to be generally produced at relatively high temperatures (>300 °C).[51,52] This further suggests that the use of hydrochars instead of pyrochars for remediation purposes as sorbents would be promising.

**Role of Amorphous Alkyl Domain of Hydrochars in Their Sorption.** The high sorption capacity of hydrochar may be tied to its distinct structure. Wang et al.[53] proposed that geosorbents of higher polarity (characterized by O/C or O+N/C or total polar functional groups) would have lower sorption for organic compounds, since they have substantial hydrophilic moieties facing outside, which can facilitate the formation of a water cluster at their surfaces through H-bonding. Water clusters would reduce the surface hydrophobicity of sorbents and the accessibility of organic molecules to sorption domains, thereby decreasing their sorption capacity. This, along with the aforementioned lower contents of surface O-containing functional groups of hydrochars (Table S3), indicates that the higher sorption capacity of hydrochars may be partly explained by their comparatively lower surface O-containing functional groups. However, the surface O-containing functional groups of hydrochars were only slightly lower than the corresponding pyrochars (Table S3) and thus were less likely to be the major factor accounting for their high sorption capacity. As discussed above, HTC resulted in hydrochar with a kerogen-like structure. With respect to kerogen, the important role of their alkyl domains in the interaction with HOCs has been highlighted before.[19,20] In our previous research,[14] it was clearly demonstrated that the alkyl C dominated the sorption of HOCs by NOM including kerogen. Hence, just like kerogen, alkyl C of hydrochars may also be the main structural components accounting for the sorption capacity. This was supported by the results for HSS250, which had a higher level of aliphaticity than HPL250 and showed a higher log $K_{oc}$ for each chemical (Tables S5−S9). The molecular flexibility of amorphous alkyl domains has been proposed to endow them with better structural compatibility with organic compounds.[54] Moreover, an overview by Chefetz and Xing[21] has also suggested that the relatively low density of the mobile amorphous alkyl regions closely resembles that of alkane solvents, and these regions can serve as an ideal medium for the sorption of HOCs. In this sense, it could be assumed that the amorphous alkyl C of hydrochars primarily accounted for their high sorption capacity to PYE and PPCPs. However, hydrochars were demonstrated to be composed of both alkyl and aryl C; the role of aryl C in the sorption of hydrochars should be further clarified. The bleaching technique, which has been previously employed to selectively degrade noncondensed aromatic moieties in organic geosorbents,[14] was used to treat the hydrochars and pyrochars. It removed substantial amounts of OC (Table S2). For the hydrochars, approximately one-third of the original OC was recovered, while the OC recovery of pyrochars ranged from 12.34% up to 55.33%. The NMR results in Figure 4b and c clearly illustrated that bleaching treatment successfully removed part of aryl C of the hydrochars, which was further supported by the significantly positive relationship between the OC mass loss and the decreased aromaticity of all samples by bleaching (Figure S4). Furthermore, Raman spectra for bleached samples showed that bleaching treatment decreased the amorphous C peak of hydrochars (Figure 3). These results revealed that the amorphous aryl C was the main component which was degraded by bleaching procedure. Table S4 presents the percentage of the removed aromatic C (amorphous aromatic C) by bleaching to the total aromatic C of their untreated counterparts. The contribution of amorphous aromatic C accounted for 78.40−79.06% to the total aromatic C of hydrochars. Moreover, we determined the log $K_{oc}$ values ($C_e$ = 0.01, 0.1 $S_w$) of bleached hydrochars to nonpolar (PYE) and polar (E1) organic contaminants. It was seen that after the removal of amorphous aryl C, the log $K_{oc}$ values of PYE and E1 by HSS250 and HPL250 were practically unchanged (Table 1). For example, log $K_{oc}$ ($C_e$ = 0.01 $S_w$) of PYE by HSS250 and HPL250 changed from 6.19 and 6.08 to 6.27 and 6.12, respectively (Table 1). It was clear that in addition to amorphous alkyl C, amorphous aryl C should also contribute to the sorption of hydrochar; otherwise the removal of amorphous aryl C and the decrease of OC after bleaching treatment should result in the increase of log $K_{oc}$ if alkyl C exclusively dominated the sorption. Moreover, amorphous aromatic C should play a comparable role in the high sorption capacity of hydrochars compared to amorphous alkyl C.

**Role of Aromatic Domains and Porosity of Pyrochars in Their Sorption.** It has been widely reported that the pore-filling mechanism plays a key role in HOC sorption by microporous solids of geosorbents in soils.[5,14] The significantly positive correlation between log $K_{oc}$ values of each sorbate for pyrochars and their $CO_2$−SA obtained in our case (Figure S3c) further supports that pore filling is a major mechanism regulating sorption interactions of HOC−pyrochars. In order to test if the pore-filling mechanism exclusively controlled sorption of these five chemicals, their log $K_{oc}$ values were normalized with the $CO_2$−SA. The values of log $K_{oc}/CO_2$−SA


DOI: 10.1021/acs.est.6b02401
Environ. Sci. Technol. 2016, 50, 13274−13282

Table 1. Log $K_{oc}$ Values ($C_e$ = 0.01 and 0.1 $S_w$) of Pyrene (PYE) and Estrone (E1) by Original and Bleached Hydrochars and Pyrochars[a]

| | log $K_{oc}$ (mL/g) | | | |
|---|---|---|---|---|
| | pyrene (PYE) | | estrone (E1) | |
| samples | $C_e$ = 0.01$S_w$ | $C_e$ = 0.1$S_w$ | $C_e$ = 0.01$S_w$ | $C_e$ = 0.1$S_w$ |
| HSS250 | 6.19 | 5.97 | 4.78 | 4.58 |
| PSS250 | 5.56 | 5.56 | 3.19 | 3.05 |
| PSS450 | 5.85 | 5.36 | 3.63 | 3.16 |
| PSS600 | 5.71 | 5.08 | 4.24 | 3.46 |
| HPL250 | 6.08 | 5.82 | 4.53 | 4.29 |
| PPL250 | 5.33 | 5.19 | 3.45 | 3.20 |
| PPL450 | 5.70 | 5.22 | 3.76 | 3.11 |
| PPL600 | 5.78 | 5.23 | 4.15 | 3.37 |
| HSS250-BL | 6.27 | 6.05 | 4.85 | 4.64 |
| PSS250-BL | 5.15 | 4.38 | 2.75 | 2.50 |
| PSS450-BL | 5.48 | 4.86 | 3.23 | 2.94 |
| PSS600-BL | 5.61 | 5.01 | 4.18 | 3.37 |
| HPL250-BL | 6.12 | 5.88 | 4.60 | 4.35 |
| PPL250-BL | 5.19 | 4.96 | 3.11 | 2.87 |
| PPL450-BL | 5.57 | 5.15 | 3.71 | 3.03 |
| PPL600-BL | 5.71 | 5.15 | 4.13 | 3.33 |

[a] $K_{oc}$ is the organic carbon (OC) normalized sorption distributed coefficient. $S_w$: aqueous solubility of pyrene (PYE) and estrone (E1). Note that H and P represent hydrochars and pyrochars, respectively. SS and PL refer to the biochars obtained from swine solids and poultry litter, respectively; 250, 450, and 600 are the heating treatment temperatures. BL: bleached samples (°C).

for the specific compounds by pyrochars at low and high HTTs still exhibited great differences, indicating that apart from the microporosity of pyrochars, other factors such as aromatic domains also affected sorption of these chemicals.

As discussed above, pyrochars, especially ones at 450 and 600 °C, mainly consisted of aromatics. It has been documented that aromatic $\pi$ systems in low-HTT pyrochars rich in electron-withdrawing functional groups will tend to be electron-deficient and thus can act as $\pi$ acceptors, and the aromatic sheets of high-HTT pyrochars may theoretically act as both electron donors and acceptors toward sorbates.[1] Among the sorbate molecules investigated, PYE has been shown to be able to behave as $\pi$-donors.[55] Also, −OH on the aromatic ring of AMP, E1, and TCS as well as $-NH_2$ in the amide group on the aromatic ring of CBZ (Table S1) are all electron-donating groups.[56,57] According to the review by Keiluweit and Kleber,[58] PYE and four PPCPs (as electron donors) could be adsorbed to the pyrochars (as $\pi$-acceptors) via $\pi-\pi$ electron donor−acceptor interactions or polar−$\pi$ interactions. These along with the strikingly positive relationship between the aromaticity of pyrochars and the log $K_{oc}$ values of each compound (Figure S3d) indicate that the sorption capacity of pyrochars for PYE and PPCPS may also result from the contribution of $\pi-\pi$ electron donor−acceptor interactions or polar−$\pi$ interactions between the sorbates and the aromatic components within pyrochars. In good agreement with this conclusion, the removal of amorphous aromatic C of pyrochars was noted to lead to the decrease in log $K_{oc}$ of PYE and TCS by pyrochars to varying degrees (Table 1).

**Environmental Implications.** In this work, we investigated the sorption capacities of hydrochars and pyrochars derived from the same manure source toward PYE and four PPCPs. Hydrochars were noted to more effectively adsorb both polar PPCPs and nonpolar PYE than pyrochars. Additionally, we observed that HTC resulted in hydrochars with kerogen-like structure whose alkyl C has already been demonstrated to be responsible for their sorption capacity. Further, it was observed that the log $K_{oc}$ values of hydrochars were almost unchanged after the removal of amorphous aryl C, implying that amorphous aromatic C played a comparable role in the high sorption capacity of hydrochars compared to amorphous alkyl C. We thus concluded that the dominant amorphous C associated with both alkyl and aryl moieties within hydrochars explained their high sorption capacity for organic pollutants. This research clearly provides evidence for mechanisms underlying the high sorption capacity of hydrochars for both nonpolar and polar organic pollutants. However, it should be noted that although the high sorption capacity of animal-manure-derived hydrochar was identified in this work, issues about the long-term environmental behavior of hydrochars, such as the release of potential toxic substances from hydrochars into soils and the stability of OC within hydrochars in soils, need to be more clearly addressed in the future before widely applying hydrochars into the environment for remediation purposes.

## ■ ASSOCIATED CONTENT

### Supporting Information

The Supporting Information is available free of charge on the ACS Publications website at DOI: 10.1021/acs.est.6b02401.

Four figures and nine tables (PDF)

## ■ AUTHOR INFORMATION


### Corresponding Author

*Phone: (86)-10-58807493. Fax: (86)-10-58807493. E-mail: sunke@bnu.edu.cn.

### ORCID

Ke Sun: 0000-0003-0425-7754


### Notes

The authors declare no competing financial interest.

## ■ ACKNOWLEDGMENTS

The authors would like to acknowledge the technical support provided by Mr. Melvin Johnson of the USDA-ARS Coastal Plains Soil, Water & Plant Research Center, Florence, SC. This research was supported by National Natural Science Foundation of China (41273106 and 41473087) and National Science Foundation for Innovative Research Group (51421065), State Education Ministry, and USDA McIntire-Stennis Program (MAS 00028). L.H. also thanks the China Scholarship Council for supporting her study at the University of Massachusetts, Amherst. Mention of trade names or commercial products is solely for the purpose of providing specific information and does not imply recommendation or endorsement by the U.S. Department of Agriculture.

## ■ REFERENCES

(1) Jin, J.; Sun, K.; Wu, F.; Gao, B.; Wang, Z.; Kang, M.; Bai, Y.; Zhao, Y.; Liu, X.; Xing, B. Single-solute and bi-solute sorption of phenanthrene and dibutyl phthalate by plant-and manure-derived biochars. *Sci. Total Environ.* **2014**, *473*, 308−316.

(2) Lattao, C.; Cao, X.; Mao, J.; Schmidt-Rohr, K.; Pignatello, J. J. Influence of molecular structure and adsorbent properties on sorption of organic compounds to a temperature series of wood chars. *Environ. Sci. Technol.* **2014**, *48*, 4790−4798.



DOI: 10.1021/acs.est.6b02401
*Environ. Sci. Technol.* 2016, 50, 13274−13282

(3) Lehmann, J.; Gaunt, J.; Rondon, M. Biochar sequestration in terrestrial ecosystems—a review. *Mitig. Adapt. Strat. Gl.* **2006**, *11* (2), 395–419.
(4) Chen, B.; Zhou, D.; Zhu, L. Transitional adsorption and partition of nonpolar and polar aromatic contaminants by biochars of pine needles with different pyrolytic temperatures. *Environ. Sci. Technol.* **2008**, *42* (14), 5137–5143.
(5) Chun, Y.; Sheng, G.; Chiou, C. T.; Xing, B. Compositions and sorptive properties of crop residue-derived chars. *Environ. Sci. Technol.* **2004**, *38* (17), 4649–4655.
(6) Keiluweit, M.; Nico, P. S.; Johnson, M. G.; Kleber, M. Dynamic molecular structure of plant biomass-derived black carbon (biochar). *Environ. Sci. Technol.* **2010**, *44* (4), 1247–1253.
(7) Cao, X.; Ro, K. S.; Libra, J. A.; Kammann, C. I.; Lima, I.; Berge, N.; Li, L.; Li, Y.; Chen, N.; Yang, J.; Deng, B.; Mao, J. Effects of biomass types and carbonization conditions on the chemical characteristics of hydrochars. *J. Agric. Food Chem.* **2013**, *61* (39), 9401–9411.
(8) Titirici, M.-M.; Antonietti, M. Chemistry and materials options of sustainable carbon materials made by hydrothermal carbonization. *Chem. Soc. Rev.* **2010**, *39* (1), 103–116.
(9) Titirici, M. M.; Thomas, A.; Yu, S.-H.; Müller, J.-O.; Antonietti, M. A direct synthesis of mesoporous carbons with bicontinuous pore morphology from crude plant material by hydrothermal carbonization. *Chem. Mater.* **2007**, *19* (17), 4205–4212.
(10) Parshetti, G. K.; Hoekman, S. K.; Balasubramanian, R. Chemical, structural and combustion characteristics of carbonaceous products obtained by hydrothermal carbonization of palm empty fruit bunches. *Bioresour. Technol.* **2013**, *135* (3), 683–689.
(11) Fuertes, A.; Arbestain, M. C.; Sevilla, M.; Maciá-Agulló, J.; Fiol, S.; López, R.; Smernik, R. J.; Aitkenhead, W.; Arce, F.; Macias, F. Chemical and structural properties of carbonaceous products obtained by pyrolysis and hydrothermal carbonisation of corn stover. *Aust. J. Soil Res.* **2010**, *48* (7), 618–626.
(12) Titirici, M.-M.; White, R. J.; Falco, C.; Sevilla, M. Black perspectives for a green future: hydrothermal carbons for environment protection and energy storage. *Energy Environ. Sci.* **2012**, *5* (5), 6796–6822.
(13) Cao, X.; Ro, K. S.; Chappell, M.; Li, Y.; Mao, J. Chemical structures of swine-manure chars produced under different carbonization conditions Investigated by advanced Solid-State $^{13}C$ Nuclear Magnetic Resonance (NMR) Spectroscopy. *Energy Fuels* **2010**, *25* (1), 388–397.
(14) Han, L.; Sun, K.; Jin, J.; Wei, X.; Xia, X.; Wu, F.; Gao, B.; Xing, B. Role of structure and microporosity in phenanthrene sorption by natural and engineered organic matter. *Environ. Sci. Technol.* **2014**, *48*, 11227–11234.
(15) Sun, K.; Jin, J.; Kang, M.; Zhang, Z.; Pan, Z.; Wang, Z.; Wu, F.; Xing, B. Isolation and characterization of different organic matter fractions from a same soil source and their phenanthrene sorption. *Environ. Sci. Technol.* **2013**, *47* (10), 5138–5145.
(16) Sun, K.; Ro, K.; Guo, M.; Novak, J.; Mashayekhi, H.; Xing, B. Sorption of bisphenol A, 17$\alpha$-ethinyl estradiol and phenanthrene on thermally and hydrothermally produced biochars. *Bioresour. Technol.* **2011**, *102* (10), 5757–5763.
(17) Guo, X.; Wang, X.; Zhou, X.; Ding, X.; Fu, B.; Tao, S.; Xing, B. Impact of the simulated diagenesis on sorption of naphthalene and 1-naphthol by soil organic matter and its precursors. *Environ. Sci. Technol.* **2013**, *47* (21), 12148–12155.
(18) Wu, L. M.; Zhou, C. H.; Tong, D. S.; Yu, W. H.; Wang, H. Novel hydrothermal carbonization of cellulose catalyzed by montmorillonite to produce kerogen-like hydrochar. *Cellulose* **2014**, *21* (4), 2845–2857.
(19) Ran, Y.; Sun, K.; Yang, Y.; Xing, B.; Zeng, E. Strong sorption of phenanthrene by condensed organic matter in soils and sediments. *Environ. Sci. Technol.* **2007**, *41* (11), 3952–3958.
(20) Schimmelpfennig, S.; Müller, C.; Grünhage, L.; Koch, C.; Kammann, C. Biochar, hydrochar and uncarbonized feedstock application to permanent grassland—Effects on greenhouse gas emissions and plant growth. *Agric., Ecosyst. Environ.* **2014**, *191*, 39–52.
(21) Chefetz, B.; Xing, B. Relative role of aliphatic and aromatic moieties as sorption domains for organic compounds: a review. *Environ. Sci. Technol.* **2009**, *43* (6), 1680–1688.
(22) Mao, J.-D.; Hundal, L.; Thompson, M.; Schmidt-Rohr, K. Correlation of poly (methylene)-rich amorphous aliphatic domains in humic substances with sorption of a nonpolar organic contaminant, phenanthrene. *Environ. Sci. Technol.* **2002**, *36* (5), 929–936.
(23) Spokas, K. A.; Novak, J. M.; Stewart, C. E.; Cantrell, K. B.; Uchimiya, M.; DuSaire, M. G.; Ro, K. S. Qualitative analysis of volatile organic compounds on biochar. *Chemosphere* **2011**, *85* (5), 869–882.
(24) Sun, K.; Gao, B.; Zhang, Z.; Zhang, G.; Zhao, Y.; Xing, B. Sorption of atrazine and phenanthrene by organic matter fractions in soil and sediment. *Environ. Pollut.* **2010**, *158* (12), 3520–3526.
(25) Sun, K.; Kang, M.; Zhang, Z.; Jin, J.; Wang, Z.; Pan, Z.; Xu, D.; Wu, F.; Xing, B. Impact of deashing treatment on biochar structural properties and potential sorption mechanisms of phenanthrene. *Environ. Sci. Technol.* **2013**, *47* (20), 11473–11481.
(26) Qiu, M.; Sun, K.; Jin, J.; Gao, B.; Yan, Y.; Han, L.; Wu, F.; Xing, B. Properties of the plant- and manure-derived biochars and their sorption of dibutyl phthalate and phenanthrene. *Sci. Rep.* **2014**, *4*, 5295–5305.
(27) Standardized product definition and product testing guidelines for biochar that is used in soil. *IBI Biochar Standards*; International Biochar Initiative, 2012.
(28) Schmidt, H.; Abiven, S.; Kammann, C.; Glaser, B.; Bucheli, T.; Leifeld, J. *Guidelines for Biochar Production*; Delinat Institute und Biochar Science Network: Arbaz, Switzerland, 2012.
(29) Singh, B. P.; Cowie, A. L.; Smernik, R. J. Biochar carbon stability in a clayey soil as a function of feedstock and pyrolysis temperature. *Environ. Sci. Technol.* **2012**, *46* (21), 11770–11778.
(30) Wu, W.; Yang, M.; Feng, Q.; McGrouther, K.; Wang, H.; Lu, H.; Chen, Y. Chemical characterization of rice straw-derived biochar for soil amendment. *Biomass Bioenergy* **2012**, *47*, 268–276.
(31) Guo, J.; Chen, B. Insights on the molecular mechanism for the recalcitrance of biochars: interactive effects of carbon and silicon components. *Environ. Sci. Technol.* **2014**, *48* (16), 9103–9112.
(32) Li, F.; Cao, X.; Zhao, L.; Wang, J.; Ding, Z. Effects of mineral additives on biochar formation: carbon retention, stability, and properties. *Environ. Sci. Technol.* **2014**, *48* (19), 11211–11217.
(33) Han, L.; Sun, K.; Jin, J.; Xing, B. Some concepts of soil organic carbon characteristics and mineral interaction from a review of literature. *Soil Biol. Biochem.* **2016**, *94*, 107–121.
(34) Malghani, S.; Jüschke, E.; Baumert, J.; Thuille, A.; Antonietti, M.; Trumbore, S.; Gleixner, G. Carbon sequestration potential of hydrothermal carbonization char (hydrochar) in two contrasting soils; results of a 1-year field study. *Biol. Fertil. Soils* **2015**, *51* (1), 123–134.
(35) Brodowski, S.; Amelung, W.; Haumaier, L.; Abetz, C.; Zech, W. Morphological and chemical properties of black carbon in physical soil fractions as revealed by scanning electron microscopy and energy-dispersive X-ray spectroscopy. *Geoderma* **2005**, *128* (1), 116–129.
(36) Ferrari, A.; Robertson, J. Resonant Raman spectroscopy of disordered, amorphous, and diamondlike carbon. *Phys. Rev. B: Condens. Matter Mater. Phys.* **2001**, *64* (7), 075414.
(37) Lehmann, J.; Joseph, S. *Biochar for Environmental Management: Science, Technology and Implementation*; Routledge, 2015.
(38) Ran, Y.; Xiao, B.; Huang, W.; Peng, P.; Liu, D.; Fu, J.; Sheng, G. Kerogen in aquifer material and its strong sorption for nonionic organic pollutants. *J. Environ. Qual.* **2003**, *32* (32), 1701–9.
(39) Petsch, S. T.; Smernik, R. J.; Eglinton, T. I.; Oades, J. M. A solid state $^{13}C$-NMR study of kerogen degradation during black shale weathering. *Geochim. Cosmochim. Acta* **2001**, *65* (12), 1867–1882.
(40) Huang, W. L.; Weber, W. J. A distributed reactivity model for sorption by soils and sediments 0.10. Relationships between desorption, hysteresis, and the chemical characteristics of organic domains. *Environ. Sci. Technol.* **1997**, *31* (9), 2562–2569.
(41) Ran, Y.; Sun, K.; Ma, X.; Wang, G.; Grathwohl, P.; Zeng, E. Y. Effect of condensed organic matter on solvent extraction and aqueous


DOI: 10.1021/acs.est.6b02401
*Environ. Sci. Technol.* 2016, 50, 13274–13282

leaching of polycyclic aromatic hydrocarbons in soils and sediments. *Environ. Pollut.* **2007**, *148* (2), 529−538.
(42) Lin, D.; Pan, B.; Zhu, L.; Xing, B. Characterization and phenanthrene sorption of tea leaf powders. *J. Agric. Food Chem.* **2007**, *55* (14), 5718−5724.
(43) Huang, L.; Boving, T. B.; Xing, B. Sorption of PAHs by aspen wood fibers as affected by chemical alterations. *Environ. Sci. Technol.* **2006**, *40* (10), 3279−3284.
(44) Xing, B.; Pignatello, J. J. Dual-mode sorption of low-polarity compounds in glassy poly (vinyl chloride) and soil organic matter. *Environ. Sci. Technol.* **1997**, *31* (3), 792−799.
(45) Schwarzenbach, R. P.; Gschwend, P. M.; Imboden, D. M. *Environmental Organic Chemistry*; John Wiley & Sons, 2005.
(46) Zhang, W.; Wang, L.; Sun, H. Modifications of black carbons and their influence on pyrene sorption. *Chemosphere* **2011**, *85* (8), 1306−1311.
(47) Hale, S.; Hanley, K.; Lehmann, J.; Zimmerman, A.; Cornelissen, G. Effects of chemical, biological, and physical aging as well as soil addition on the sorption of pyrene to activated carbon and biochar. *Environ. Sci. Technol.* **2011**, *45* (24), 10445−10453.
(48) Zhu, X.; Liu, Y.; Luo, G.; Qian, F.; Zhang, S.; Chen, J. Facile fabrication of magnetic carbon composites from hydrochar via simultaneous activation and magnetization for triclosan adsorption. *Environ. Sci. Technol.* **2014**, *48* (10), 5840−5848.
(49) Zhao, L.; Cao, X.; Mašek, O.; Zimmerman, A. Heterogeneity of biochar properties as a function of feedstock sources and production temperatures. *J. Hazard. Mater.* **2013**, *256*, 1−9.
(50) Sun, Y.; Gao, B.; Yao, Y.; Fang, J.; Zhang, M.; Zhou, Y.; Chen, H.; Yang, L. Effects of feedstock type, production method, and pyrolysis temperature on biochar and hydrochar properties. *Chem. Eng. J.* **2014**, *240*, 574−578.
(51) Qiu, M.; Sun, K.; Jin, J.; Han, L.; Sun, H.; Zhao, Y.; Xia, X.; Wu, F.; Xing, B. Metal/metalloid elements and polycyclic aromatic hydrocarbon in various biochars: The effect of feedstock, temperature, minerals, and properties. *Environ. Pollut.* **2015**, *206*, 298−305.
(52) Keiluweit, M.; Kleber, M.; Sparrow, M. A.; Simoneit, B. R.; Prahl, F. G. Solvent-extractable polycyclic aromatic hydrocarbons in biochar: influence of pyrolysis temperature and feedstock. *Environ. Sci. Technol.* **2012**, *46* (17), 9333−9341.
(53) Wang, X.; Guo, X.; Yang, Y.; Tao, S.; Xing, B. Sorption mechanisms of phenanthrene, lindane, and atrazine with various humic acid fractions from a single soil sample. *Environ. Sci. Technol.* **2011**, *45* (6), 2124−2130.
(54) Zhang, D.; Pan, B.; Cook, R. L.; Xing, B. Multi-walled carbon nanotube dispersion by the adsorbed humic acids with different chemical structures. *Environ. Pollut.* **2015**, *196*, 292−299.
(55) Chefetz, B.; Deshmukh, A. P.; Hatcher, P. G.; Guthrie, E. A. Pyrene sorption by natural organic matter. *Environ. Sci. Technol.* **2000**, *34* (14), 2925−2930.
(56) Oleszczuk, P.; Pan, B.; Xing, B. Adsorption and desorption of oxytetracycline and carbamazepine by multiwalled carbon nanotubes. *Environ. Sci. Technol.* **2009**, *43* (24), 9167−9173.
(57) Lin, D.; Xing, B. Adsorption of phenolic compounds by carbon nanotubes: role of aromaticity and substitution of hydroxyl groups. *Environ. Sci. Technol.* **2008**, *42* (19), 7254−7259.
(58) Keiluweit, M.; Kleber, M. Molecular-level interactions in soils and sediments: the role of aromatic π-systems. *Environ. Sci. Technol.* **2009**, *43* (10), 3421−3429.


DOI: 10.1021/acs.est.6b02401
*Environ. Sci. Technol.* 2016, 50, 13274−13282